ChemElectroChem

Research Article
doi.org/10.1002/celc.202400667

Chemistry Europe
European Chemical Societies Publishing

www.chemelectrochem.org

Aptamer-Driven Biosensor Technology for the Quantitative Analysis of C-Reactive Protein

Marlon Oranzie,*[a] Jaymi L. January,[a] Nelia A. Sanga,[a] Zandile D. Leve,[a] Sixolile Mini,[a] Candice Cupido,[a] Samantha F. Douman,*[a, b] and Emmanuel I. Iwuoha*[a]

C-reactive protein (CRP) is a widely recognized biomarker for early myocardial infarction (MI) detection, released into the bloodstream during heart inflammation. Traditional assays for CRP detection, like ELISA and immunoradiometric assays, are costly, time-consuming, and require large sample volumes. Aptasensors are becoming increasingly popular for MI diagnosis due to their affordability, simplicity, and potential for point-of-care use. In this study, an electrochemical aptasensor incorporating mercaptosuccinic acid-capped nickel selenide quantum dots (MSA-$NiSe_2$ QD) were developed for CRP detection. The amine-modified aptamer was immobilized on the MSA-$NiSe_2$ QD using EDC/NHS coupling chemistry. Chronocoulometric measurements showed high selectivity towards CRP in phosphate buffer, with a linear range of 10–110 pg/mL and a detection limit of 2.80 pg/mL. Cross-reactivity experiments confirmed the aptasensor's high selectivity for CRP. Testing in human serum samples demonstrated recovery rates of 94–100.5 %, indicating its suitability for clinical diagnostics. Validation studies with a commercial CRP ELISA kit showed the aptasensor's superior sensitivity in both physiological buffer and human serum.

1. Introduction

Myocardial infarction (MI) is a concern for many countries across the world. Myocardial infarction is responsible for 32 % of all deaths worldwide as reported by the World Health Organization (WHO).[1,2] The traditional techniques for diagnosing patients with MI include electrocardiograms (ECGs) and blood tests.[3,4] The problems with these techniques are they are expensive, waiting on results is time-consuming and it is invasive for patients. Therefore, biomarkers are required to monitor and provide effective treatments for patients suffering from MI. Biomarkers are biological molecules found in bodily fluids and blood that measure the presence or progress of diseases.[5,6] C-reactive protein (CRP) is a biomarker for MI and is released into the bloodstream due to the inflammation of the heart.[7] The American Heart Organization states that the normal concentration of CRP in the bloodstream is 1 ng/mL and anything above 5 ng/mL is considered a high risk for a myocardial infarct attack.[8] Most detection techniques investigated for CRP include kit-based models such as enzyme-linked immunosorbent assay (ELISA) and fluorescence spectroscopy. These techniques are efficient and can detect CRP at picomolar levels, but they are time-consuming, costly, and necessitate huge sample volumes.[9] Therefore, research today is focused more on electrochemical biosensors due to the fact they are inexpensive, portable, require small sample volumes and are highly sensitive.[10] Most electrochemical detection methods reported for CRP in literature are immuno-based methods which are an antibody-antigen recognition system.[11] The problems with immuno-based sensors are that the antibodies are expensive to produce, they can undergo non-specific binding with foreign molecules and can lead to depuration from the bound label.[12] Therefore, aptasensors are being researched as an alternative detection protocol to immuno-based sensors. The systematic evolution of ligands by exponential enrichment (SELEX) technology is used to make single-stranded DNA or RNA oligonucleotides called aptamers that are intended to bind and recognize targets.[13] Aptamers are preferable to antibodies because of their high specificity, affinity, stability, ease of modification, and low cost of production.[14] The aptasensor can be enhanced with nanomaterials like quantum dot (QD), gold nanoparticles, and carbon nanotubes, as these materials increase the sensitivity and specificity of the sensor because of their large surface area and high conductivity.[15] Wang et al.[16] developed an RNA-based electrochemical aptasensor incorporating silica microspheres for the detection of CRP. The microspheres enhanced the analytical signal of the sensor due to its large surface area and the sensor had a linear range of 0.005 ng/mL to 125 ng/mL and a limit of detection (LOD) of 0.017 ng/mL. The sensor was applied in real sample analysis and achieved a percentage recovery ranging from 91.1 to 103 % which makes the sensor suitable for clinical applications for the

[a] M. Oranzie, J. L. January, N. A. Sanga, Z. D. Leve, S. Mini, C. Cupido, S. F. Douman, E. I. Iwuoha
SensorLab (University of the Western Cape Sensor Laboratories), Chemical Sciences Building, University of the Western Cape, Bellville 7535, Cape Town, South Africa
E-mail: 3338704@myuwc.ac.za
samantha.douman@uct.ac.za
eiwuoha@uwc.ac.za

[b] S. F. Douman
Department of Chemistry, University of Cape Town, Rondebosch, Cape Town, 7700, South Africa

Supporting information for this article is available on the WWW under https://doi.org/10.1002/celc.202400667

detection of CRP. In another study Tabrizi el al.[17] developed an RNA-based electrochemical aptasensor for the detection of CRP using carbon nanofiber-chitosan modified screen printed electrode. The carbon nanofiber-chitosan was used to enhance the electrochemical signal as well as increase the surface coverage of the aptamer. Square wave voltammetry (SWV) was used as a detection technique and the sensor was able to detect CRP over a wide linear range of 23 –3450 pg/mL and achieved a LOD of 8.51 pg/mL. This research study focuses on the fabrication of an electrochemical aptasensor incorporating mercaptosuccinic capped nickel selenide quantum dots (MSA-$NiSe_2$ QD) for the detection of CRP in physiological buffer and human serum in real time. The MSA-$NiSe_2$ QD is incorporated on the screen-printed carbon electrode (SPCE) via an electrografting method followed by immobilization of the amine-modified aptamer through cross-linking chemistries for detection of CRP via chronocoulometry (CC).

Experimental

Chemical and Reagents

The full list of the chemical reagents and instrumentation used are shown in detail in the supplementary material. The aptamer with the sequence the 5′ amino modified aptamer (sequence:5′-NH_2GCCTGAAGGTGGTCGGTGTGGCGAGTGTGTTAGGAGAGATTGC-3′) with a dissociation constant of 33.34 ± 1.15 nM was first produced by Li and co-workers[18] and purchased from Integrated DNA Technologies Inc. (Coralville, IA, USA).

Synthesis of MSA-$NiSe_2$ QD

The MSA-$NiSe_2$ QD was prepared as described by Marlon and co-workers with full details described in the supplementary document.[19]

Electrochemical Grafting of 4 Nitrophenyl Layers on SPCEs

Nitrophenyl groups were formed on the screen-printed carbon electrode (SPCE) surface through an in situ diazonium cation process by mixing a solution containing 2.0 mM $NaNO_2$ and 1.0 mM of 4-nitroanaline and 0.5 M HCl, it was possible to. The mixture was subsequently left to react for 5 minutes at room temperature. The SPCE was drop-coated with 50 μL of the solution and linked to a PalmSens electrochemical workstation. Cyclic voltammetry (CV) was conducted, scanning from +0.7 V to −0.4 V at a rate of 0.05 V/s. The nitro-modified SPCE was then rinsed with deionized water. To reduce the nitro groups to amine groups, CV was performed again, scanning from 0 V to −1.2 V at 0.05 V/s in a 1.0 M KCl solution. Finally, the amine-modified SPCE was washed with deionized water for aptasensor fabrication.

Aptasensor Fabrication

Scheme 1 depicts the fabrication process of the CRP sensor. After electrographting the SPCE was subjected to 1-ethyl-3-(3-dimethylaminopropyl) carbodiimide/N-hydroxysuccinimide (EDC/NHS) cross-linking chemistries for 30 min at room temperature for activation of

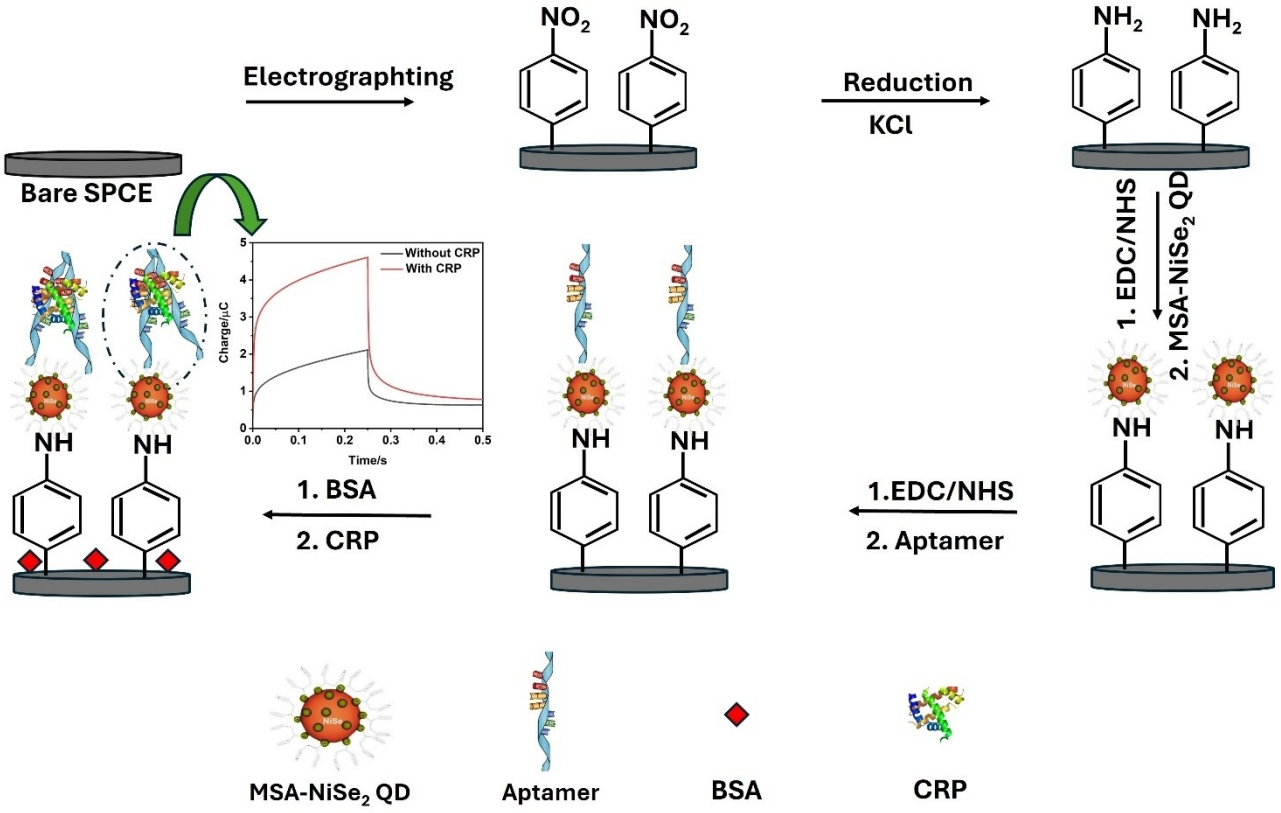

Scheme 1. Illustration for the fabrication of the CRP aptasensor.

the amine groups to bind covalently to the carboxyl functionalized QD. Once the QD were drop coated on the SPCE it was left to react overnight in a dark environment. The SPCE/QD was then activated with EDC/NHS for 30 min to activate the free carboxyl groups of the QD to covalently bind to the amine-modified aptamer. Once the aptamer was drop coated on the SPCE/QD it was left in the fridge for 24 h. The SPCE/QD/Apt was then blocked with BSA for 30 min to block non-specific sites on the electrode surface. The SPCE/QD/Apt/BSA sensor was then ready for CRP detection. It should be noted that 50 μL of each reagent was added onto the electrode surface and after each step; the electrode was rinsed with dulbecco phosphate buffer saline (DPBS, pH 7.4).

Chronocoulometric Detection

CRP was measured electrochemically using choronocoulometry (CC) in 10 mM dulbecco phosphate buffer saline (DPBS) (pH 7.4) at room temperature. Choronocoulometry was used as a detection technique since it has a fast signal readout of 10 s, which is advantageous over other electrochemical techniques such as cyclic voltammetry (CV), square wave (SWV), and differential pulse voltammetry (DPV). These advantages make it suitable for real-time analysis for sensor applications. The concentration of the CRP was directly proportional to the charge generated in choronocoulometry and this was used to generate the curve of calibration. In this work, different standard CRP concentrations were spiked in phosphate buffer solution and were detected using the aptasensor. The investigation of the selectivity and stability of the sensor followed the same methodology.

Various analytes, including L-cysteine, troponin I (cTnI), and bovine albumin serum (BSA), were compared to CRP in the selectivity investigation. Human serum was used for real-world sample analysis. Before usage, the serum sample was diluted in a 1 : 10 ratio with 10 mM DPBS (pH 7.4). The serum sample was then spiked with different CRP concentrations.

2. Results and Discussion

2.1. Optimization of the Aptasensor

Parameters affecting the sensitivity of the aptasensor were investigated such as the aptamer concentration, aptamer incubation time, different blocking buffers and accumulation time. In Figure 1A different aptamer concentrations were investigated ranging from 1 μM to 6 μM. It can be observed that there is a steady increase in the peak charge with increasing aptamer concentration and after 5 μM the charge remains constant which is an indication that the saturation of the aptamer has been reached. Therefore 5 μM was chosen as the optimum concentration as it displays the highest peak charge before saturation. In Figure 1B the aptamer incubation time was investigated to determine the total amount of time for the aptamer to bind to the electrode surface and produce the highest peak charge before saturation. A lengthy incubation with oligonucleotides is thought to decrease non-specific binding between the aptamer probe and the transducer surface.[20] It can be observed that the peak charge increases at a steady rate for the first 12 h after 12 h the saturation of the aptamer occurs, and the peak charge remains constant. Therefore 12 h was chosen as the optimum aptamer incubation time.

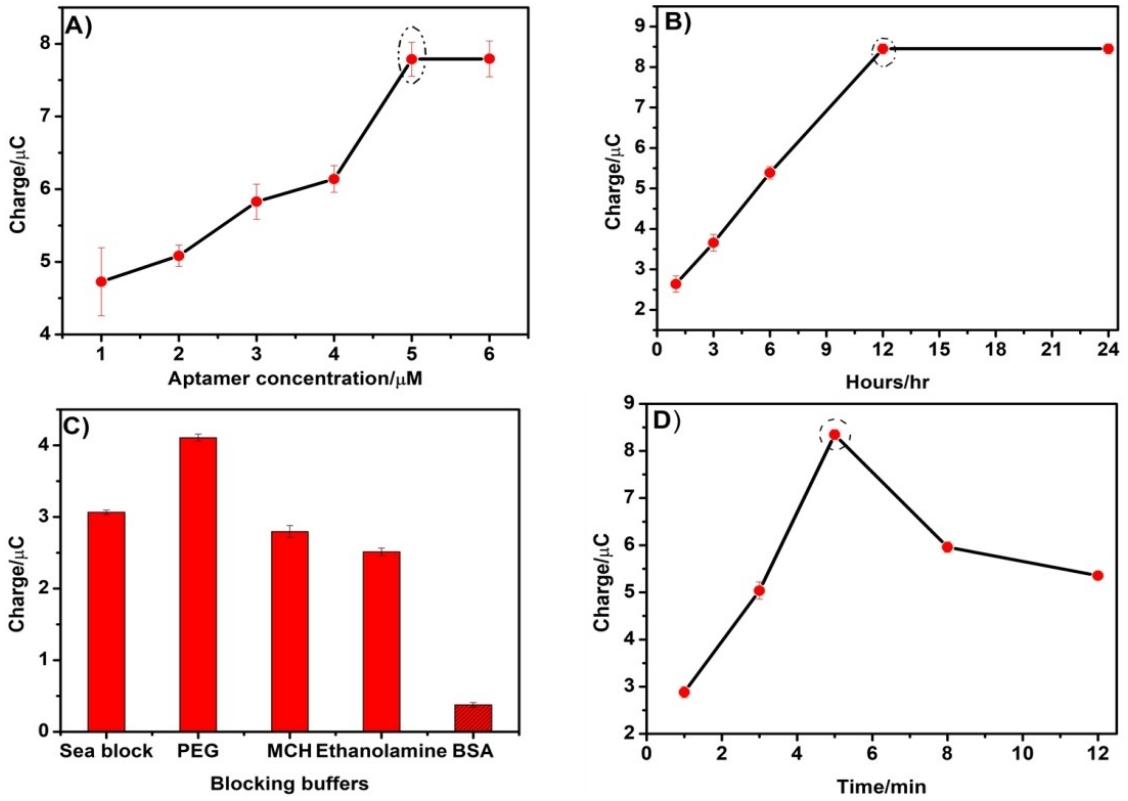

Figure 1. Optimization of A) aptamer concentration B) aptamer incubation time C) blocking buffers D) Accumulation time in 10 mM DPBS, pH 7.4.

Another parameter investigated in Figure 1C was the effect of different blocking buffers such as sea block, polyethylene glycol (PEG), mercaptohexanol (MCH), ethanolamine and bovine albumin serum (BSA) on the aptasensor. This experiment aimed to determine the blocking buffer that displays the lowest peak charge as it blocks all non-specific binding sites of the aptasensor and this in turn slows down the transfer of electrons and leads to a lower peak charge. BSA was chosen as the suitable blocking buffer for the sensor as it displayed the lowest peak charge. The final parameter investigated was the accumulation time as displayed in Figure 1D from 1 to 12 min. The accumulation time is the amount of time it takes for the complete binding between the aptamer and the analyte, and it is displayed as an increase in peak charge.[21] It can be observed that 5 min had the highest peak charge compared to the other times chosen and thus was selected as the ideal duration for the aptamer and analyte to fully bind prior to detection.

2.2. Determination of Aptamer Surface Density, Γ_{DNA}

The aptamer surface density was determined by calculating the surface density of the sensor with QD and without the presence of QD and just the aptamer alone (done through electrographting carboxyl groups directly on the SPCE) in 0.1 M $[Ru(NH_3)_6]^{3+}$. The surface density can be determined based on the electrostatic interaction of the negatively charged phosphate backbone of the aptamer and the positively charged RuHex probe. The surface density could then be obtained using the integrated Cottrell equation from data obtained from the chronocoulogram.[22] The Cottrell equation:

$$\Gamma^{-0} = \frac{Q}{nFA} \quad (1)$$

$$\text{Then, } \Gamma_{DNA} = \Gamma^{-0}\left(\frac{Z}{m}\right)(N_A) \quad (2)$$

where Γ^{-0} is the surface excess (excess amount of the redox probe present at the surface of the material) of the redox marker, Q is the charge of the redox marker estimated from the chronocoulometric graph in the presence and without the presence of QD, n is the number of electrons transferred, F is Faraday's constant, A is the microscopic area of the electrode, Γ_{DNA} is the surface coverage of aptamer, z is the charge of the redox probe $[Ru(NH_3)_6]^{3+}$, m is the number of bases in the aptamer, and N_A is Avogadro's number.

The surface density of the SPCE-Apt-QD and SPC-Apt was calculated to be 5.86×10^{13} molecules cm^{-2} and 1.08×10^{13} molecules cm^{-2} respectively. These results suggest that incorporating the QD into the aptasensor platform enhances its loading capacity by five times compared to using the aptamer only, thanks to the QD's large surface area.

2.3. Chronocoulometric and Electrochemical Impedance Behaviour of the Modified Screen-Printed Electrode Interface

Chronocoulometry (CC) and impedance (EIS) were used as an indicator for the modification of the electrode interface.[23]

It's observed from Figure 3A there that is an increase in charge from (curve a) SPCE which had a charge of 1.16 μC to (curve b) SPCE-QD which had a charge of 8.53 μC. This is due to the QD being conductive and increasing the flow of electrons thus increasing the peak charge.[24] In addition, this statement is supported by comparing the electroactive surface area (ECSA) of the Bare SPCE with the SPCE-QDs (Figure S1) which was

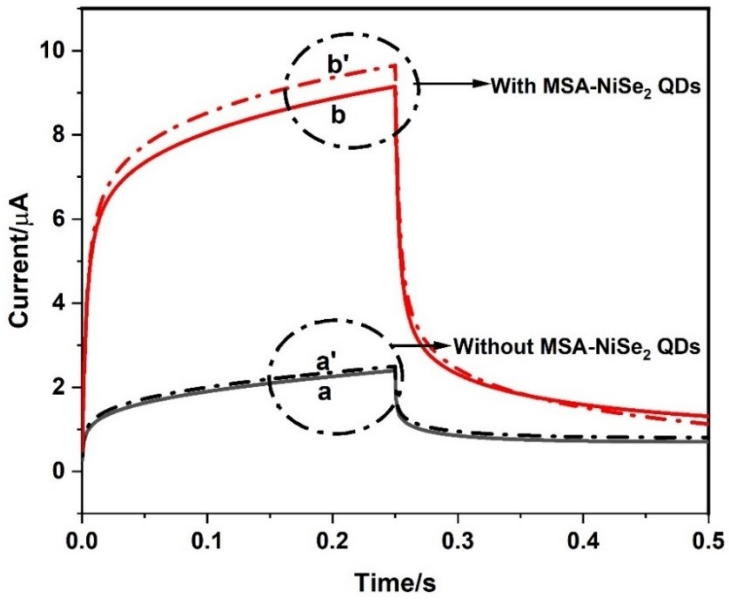

Figure 2. Chronocoulograms of the aptasensor sensor prepared without the MSA-$NiSe_2$ QDs in the absence (a) and presence (a') of $[Ru(NH_3)_6]^{3+}$. Chronocoulograms of the aptasensor prepared with the MSA-$NiSe_2$ QDs in the absence (b) and presence (b') of $[Ru(NH_3)_6]^{3+}$.

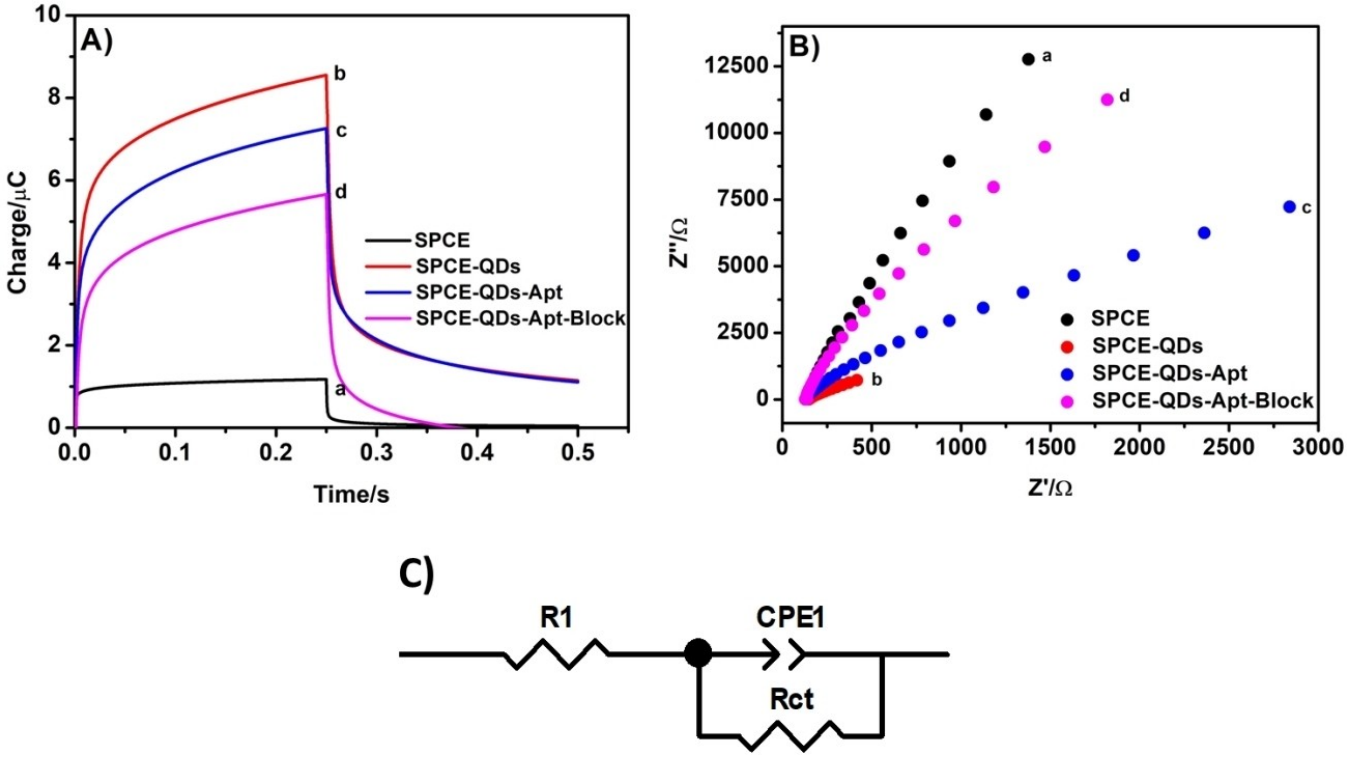

Figure 3. The electrochemical characterization of the modified electrodes: CC (A) and EIS (B) of SPCE (curve a), SPCE-QD (curve b), SPCE-QD-Apt (curve c), and SPCE-QD-Apt-block (curve d) measured in 10 mM DPBS, pH 7.4. (C) Randles equivalent circuit.

1.872 cm^2 and 2.963 cm^2 respectively. This was done using the Randels Sevcik equation:

$$I_p = 2.69 \times 10^5 A D^{\frac{1}{2}} n^{\frac{1}{3}} \nu^{\frac{1}{2}} C \quad (3)$$

where I_p represents the peak current (μA), n is the number of electrons, A is the electrode surface area (cm^2), D is the diffusion coefficient ($cm\ s^{-1}$), and ν is the scan rate (VS^{-1}). The ESCA of the SPCE-QDs was 1.5 times higher than that of the Bare SPCE and supports the increase in charge observed in Figure 3A (red line). The charge then decreases at (curve c) SPCE-Q-APT to 7.25 μC. This could be due to the electrostatic repulsion between the negatively charged carboxyl groups on the QD and the negative phosphate backbone of the aptamer.[25] There is a further decrease in peak charge at (curve d) SPCE-QD-Apt-Block which had a peak charge of 5.66 μC. This is due to the role of the blocking buffer that blocks all non-specific binding sites, which slows down the transfer of electrons and thus decreases the peak charge.[26]

In Figure 3B it can be observed that the charge transfer (R_{ct}) decreases from 793 Ω to 280 Ω respectively when the QD are applied this is because the QD are conductive and lead to less charge transfer resistance. When the aptamer is applied there is an increase in R_{ct} to 569 Ω this is because of the insulating properties that occur due to the interaction between the QD and aptamer. Finally, when the blocking buffer is added to the electrode interface the R_{ct} increases to 765 Ω due to the blocking of non-specific binding sites which hinders electron transfer and in turn, leads to an increase in charge transfer resistance.

2.4. Chronocoulometric Detection of CRP

Here, the detection of CRP was investigated using choronocoulometry (CC) as shown in Figure 4A. The CC experiments were performed in DPBS, pH 7.4 and the detection of CRP was determined based on the change observed with the change in the charge response signal with each addition of CRP. It can be observed from Figure 4A that there is an increase in charge with each addition of CRP. This might be attributed to the aptamer binding to the CRP biomarker through an electrostatic attraction between the aptamer's negative phosphate backbone and the positively charged monomeric isoform of the CRP biomarker, forming a CRP-aptamer complex.[27] The CRP-aptamer complex occurs due to the conformational change the aptamer undergoes once it binds to the biomarker. This conformational change occurs close to the electrode surface and with each addition of CRP, there is an increase in the charge response.[28] This was further supported by Figure S2 where a controlled experiment was performed to investigate the sensor's behaviour towards the detection of DPBS without the addition of the CRP analyte and it was observed that the signal increase was $<1\%$ further proving that the sensor's detection for DPBS was negligible and instead the CRP analyte was being detected by the aptasensor. Furthermore, the corresponding calibration curve in Figure 4B indicated a linear

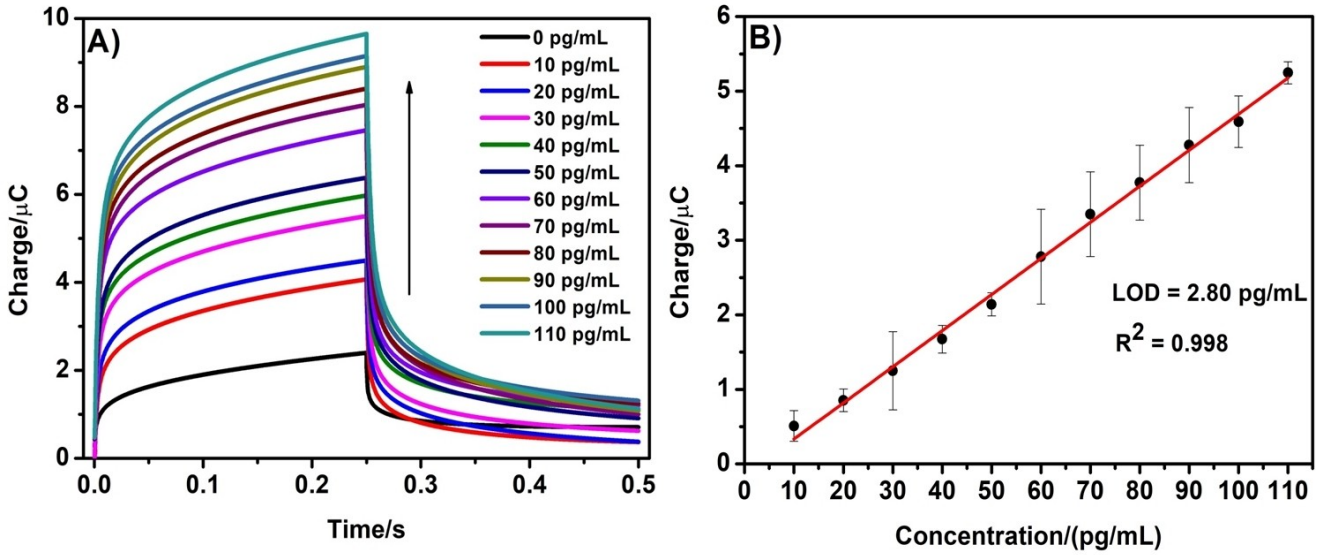

Figure 4. Chronocoulometric detection of CRP A) corresponding calibration plot B) in 10 mM DPBS, pH 7.4.

relationship due to the change in charge with each addition of the CRP biomarker in the range of 10–110 pg/mL. A linear regression of $R^2 = 0.998$ with a limit of detection (LOD) achieved was 2.80 pg/mL for (S/N = 3). Thus, it can be said that the aptasensor achieved a limit of detection much lower than the clinical cut-off value for CRP which is approximately 5.2 ng/mL. Therefore, the aptasensor displayed a satisfactory performance for detecting CRP as its LOD falls below the clinical cut-off range used to diagnose patients suffering from MI associated with CRP.

A comparison study of the aptasensor to a commercially available ELISA kit for CRP was also done in Figure 5. It could be observed that the ELISA kit had a LOD of 8.39 pg/mL which was three times higher than the aptasensor. Thus, it proves that the aptasensor is more sensitive than the commercially available ELISA kit for CRP and can be applied in clinical applications for CRP. The sensitivity of the electrochemical aptasensor could also be validated by the fact more aptamer binds to the large surface area of the QD. This was confirmed by calculating the aptamer's surface density using the integrated Cottrell equation and data from the chromatogram in Figure 2.[29] Below in

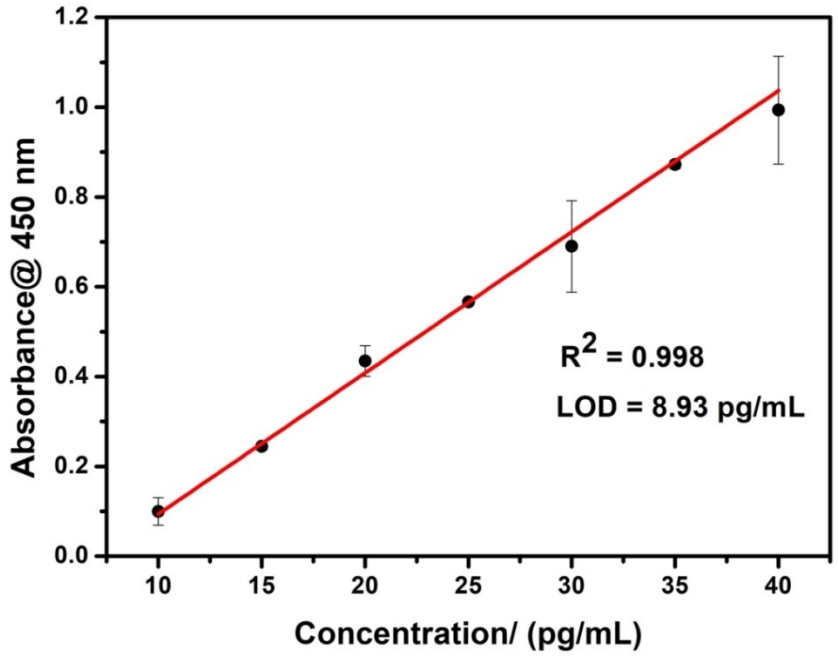

Figure 5. ELISA assay calibration plot for CRP.

Table 1 is a comparison of the parameters of the CRP aptasensor of this work with those of other CRP biosensors reported in the literature.[30–37] It can be observed from the table that we achieved a low LOD compared to previous biosensor studies for CRP. This could be due to the chalcogenide quantum dot amplification of the sensitivity of the aptasensor.

2.5. Selectivity and Stability of the Aptasensor

Selectivity studies were done on the aptasensor to investigate the effect of other interferences such as L-cysteine, BSA, cTnI and CRP. Here the interferences were incubated on the aptasensor in DPBS. From Figure 6A when compared to the blank (control), the other interferences have little to no impact on the peak charge. It can be observed that the charge for CRP increases significantly when compared to the blank. This suggests that the sensor is particularly sensitive to this protein. In addition, stability studies were done over 15 days to investigate any change in peak charge over these consecutive days. In this proposed work the aptasensor was stored at 4 °C and a 100 pg/mL of CRP was incubated on the electrode surface. Figure 6B shows that the charge was steady for the first 9 days and that the sensor kept around 100% of its initial response. From day 12 to day 15 the charge response starts to decrease to about 3% from its original charge response. Inferring that the aptasensor had good stability, therefore it can be said that the sensor kept roughly 97% of the initial charge response after 15 days.

2.6. CRP Detection in Synthetic Human Serum

To further validate the aptasensor for implementation in clinical applications, CRP was detected in synthetic human serum samples and compared to the standard ELISA kit. The serum samples were diluted in a 1:10 ratio with 10 mM DPBS, pH 7.4. Various concentrations of CRP were spiked in the serum solution ranging from 10 pg/mL to 60 pg/mL. The recovery % was computed and displayed in Table 2. Data extrapolated from the calibration curve was used to determine the percentage recovery. The table clearly shows that the aptasensor detected

Table 1. Comparison with other CRP aptasensors and immunosensors.

Method	Platform	Technique	Linear range (pg/mL)	LOD (pg/mL)	Reference
Immunosensor	IrNPs/GO/Ab_1/BSA/GCE	DPV	0.01–1000	4	[30]
Aptasensor	CNFs/CHIT/Apt/MCH/SPCE	DPV	1–3500	21.5	[31]
Aptasensor	Apt/BSA/AuE	SWV	23–2000	10	[32]
Immunosensor	ZnO/MPC/Ab_1/BSA/CPE	DPV	0.01–2000	5	[33]
Immunosensor	AuNPs/CoFe/N-GCT/Ab_1/BSA/GCE	DPV	0.5–2000	16.7	[34]
Immunosensor	AuNPs/L-cyst/Ab_1/BSA/SPCE	SWV	10–500	15	[35]
Immunosensor	AuNPs@BP@PDA/Ab1/MCH/AuE	EIS	0–36000	700	[36]
Aptasensor	AuNPs/GO-COOH/Apt/BSA/SPCE	DPV	1–100000	10	[37]
Aptasensor	MSA-$NiSe_2$ QD/Apt/BSA/SPCE	CC	10–110	2.80	This work

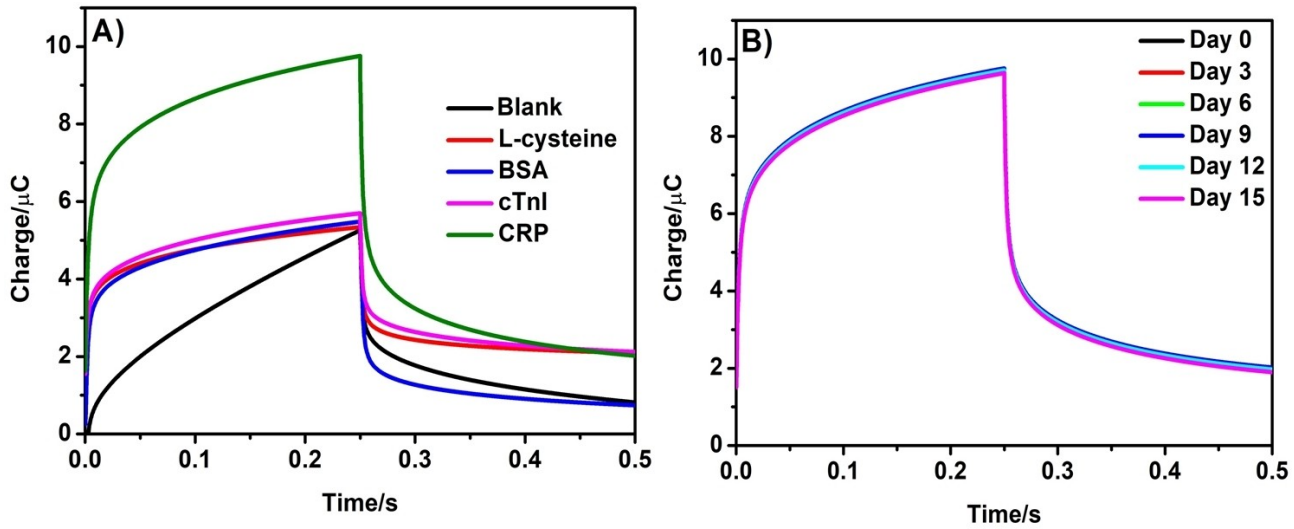

Figure 6. A) Selectivity of the CRP aptasensor. Interfering agents L-cysteine, BSA and cTnI (150 pg/mL) B). Stability studies of the aptasensor over 15 days in 10 mM DPBS.

Table 2. Percentage recovery of CRP in synthetic human serum.

CRP aptasensor					CRP by ELISA			
Serum Samples	Spiked (pg/mL)	Detected (pg/mL)	Recovery (%)	RSD (%)	Spiked (pg/mL)	Detected (pg/mL)	Recovery (%)	RSD (%)
1	10	9.98	99.8	2.1	10	9.87	98.7	3.6
2	20	28.9	94.7	3.2	20	27.9	94.6	3.9
3	40	39.7	100.5	2.7	40	46.5	94.1	4.1

CRP with a percentage recovery of 94.7–100.5 % and the ELISA kit had an average recovery percentage of 94.1–98.7 % in serum samples. It is observed that the sensor has a slighter higher percentage recovery than the commercial ELISA kit and thus can be applied in clinical applications for CRP detection.

3. Conclusions

In this study, we demonstrated the successful preparation of an electrochemical aptasensor for the detection of CRP incorporating mercaptosuccinic acid capped nickel selenide quantum dot (MSA-$NiSe_2$ QD) as it is highly sensitive, highly stable and provides a large surface area for the immobilization of aptamers. Compared to commercially available assays for CRP this aptasensor requires small sample volumes, it has a short assay time, high portability and it has multiplexing abilities. The MSA-$NiSe_2$ QD aptasensor binded to the CRP biomarker through an binding interaction and it was evaluated in phosphate buffer and human serum. The sensor achieved a low limit of detection of 2.80 pg/mL, had a fast response time and showed a satisfactory performance in synthetic human serum achieving an average percentage recovery of 94.7–100.5 %. The aptasensor also showed excellent selectivity toward CRP with no considerable cross-reactivity with other interferents. Subsequently, the stability of the aptasensor was also evaluated and the experimental results proved that the sensor could be stored for more than a week at 4 °C. This aptasensing platform has multiple benefits, including simplicity, cost-effectiveness, and high sensitivity and specificity. Compared to the ELISA, the aptasensor demonstrates a lower detection limit in both buffer and serum, making it a promising tool for clinical applications in CRP analysis.

CRediT Author Statement

Marlon Oranzie: Investigation, Formal analysis, Writing an original draft, Funding acquisition; Samantha F. Douman: Conceptualization, Methodology, Supervision, Review & editing; Jaymi L. January: Review and editing; Nelia A. Sanga: Review and editing; Zandile D. Leve: Review and editing; Sixolile Mini: Review and editing; Candice Cupido: Review and editing; Emmanuel I. Iwuoha: Conceptualization, Methodology, Project administration, Supervision, Resources, Review & editing.

Acknowledgements

The authors are grateful for the financial support from the National Research Foundation (NRF) of South Africa.

Competing Interest

The authors declare that they have no known competing financial interests or personal relationships that could have appeared to influence the work reported in this paper.

Data Availability Statement

The data that support the findings of this study are available from the corresponding author upon reasonable request.

Keywords: Chronocoulometry (CC) · C-reactive protein (CRP) · Electrochemical aptasensor · Myocardial infarction (MI) · Quantum dot (QD)

[1] Z. Gerdan, Y. Saylan, A. Denizli, *ACS Omega* **2024**, *9*, 9946.
[2] Y. Mei, X. Lin, C. He, W. Zeng, Y. Luo, C. Liu, Z. Liu, M. Yang, Y. Kuang, Q. Huang, *Front. Bioeng. Biotechnol.* **2022**, *10*, 952510.
[3] H. O. Kaya, A. E. Cetin, M. Azimzadeh, S. N. Topkaya, *J. Electroanal. Chem.* **2021**, *12*, 114.
[4] T. Dong, W. Zhu, Z. Yang, N. M. Matos Pires, Q. Lin, W. Jing, L. Zhao, X. Wei, Z. Jiang, *Biosens. Bioelectron.* **2024**, *255*, 116090.
[5] P. McGranaghan, A. Saxena, M. Rubens, J. Radenkovic, D. Bach, L. Schleußner, B. Pieske, F. Edelmann, T. D. Trippel, *Biomarkers* **2020**, *25*, 101.
[6] J. Wu, H. Liu, W. Chen, B. Ma, H. Ju, *Nat. Rev. Bioeng.* **2023**, *1*, 346.
[7] M. F. Siddiqui, Z. A. Khan, S. Park, *Nanomaterials* **2020**, *10*, 1.
[8] M. Shokripour, N. Omidifar, K. Salami, M. Moghadami, B. Samizadeh, *Canadian J. Infectious Diseases Med. Microbiol.* **2022**, *6*, 8.
[9] K. V. Mokwebo, S. F. Douman, O. V. Uhuo, K. C. Januarie, M. Oranzie, E. I. Iwuoha, *J. Electroanal. Chem.* **2022**, *920*, 116621.
[10] T. A. Tabish, H. Hayat, A. Abbas, R. J. Narayan, *Biosensors* **2024**, *12*, 77.
[11] A. Pourali, M. R. Rashidi, J. Barar, G. Pavon-Djavid, Y. Omidi, *TrAC Trends Anal. Chem.* **2021**, *134*, 116123.
[12] S. Vasantham, R. Alhans, C. Singhal, S. Nagabooshanam, S. Nissar, T. Basu, S. C. Ray, S. Wadhwa, J. Narang, A. Mathur, *Biomed. Microdevices* **2022**, *22*, 408.
[13] M. Prante, E. Segal, T. Scheper, J. Bahnemann, J. Walter, *Biosensors* **2021**, *10*, 16.
[14] L. Hosseinzadeh, M. Mazloum-Ardakani, *Advances in Aptasensor Technology*, Elsevier Inc., **2020**, *99*, 237.
[15] G. Evtugyn, A. Porfireva, R. Shamagsumova, T. Hianik, *Chemosensors* **2020**, *8*, 1.
[16] J. Wang, J. Guo, J. Zhang, W. Zhang, Y. Zhang, *Biosens. Bioelectron.* **2017**, *95*, 100.
[17] M. A. Tabrizi, P. Acedo, *Nanomaterials* **2022**, *12*, 1.
[18] H. H. Li, C. Y. Wen, C. Y. Hong, J. C. Lai, *RSC Adv.* **2017**, *7*, 42856.

[19] M. Oranzie, S. F. Douman, O. V. Uhuo, K. V. Mokwebo, N. Sanga, E. I. Iwuoha, *Analyst* **2022**, *147*, 4829.
[20] Y. Song, M. Xu, Z. Li, L. He, M. Hu, L. He, Z. Zhang, M. Du, *Sens. Actuators B* **2020**, *321*, 128527.
[21] D. Ding, C. Yang, C. Lv, J. Li, W. Tan, *Anal. Chem.* **2020**, *92*, 4108.
[22] M. M. Radhi, Y. K. A. Amir, S. H. Alwan, T. W. Tee, *J. Phys. Conf. Ser.* **2019**, *431*, 1.
[23] K. Dziąbowska, E. Czaczyk, D. Nidzworski, *Biosensors (Basel).* **2018**, *12*, 58.
[24] M. Tertiş, B. Ciui, M. Suciu, R. Săndulescu, C. Cristea, *Electrochim. Acta* **2017**, *258*, 1208.
[25] O. Uhuo, T. Waryo, M. Oranzie, N. Sanga, Z. Leve, J. January, Z. Tshobeni, K. Pokpas, S. Douman, E. Iwuoha, *Bioelectrochemistry* **2024**, *158*, 108693.
[26] Y. Liu, Q. Zhou, A. Revzin, *Analyst* **2022**, *138*, 4321.
[27] N. A. Sanga, M. Oranzie, Z. Leve, K. C. Januarie, K. V. Mokwebo, O. V. Uhuo, N. Ross, S. F. Douman, K. Pokpas, E. I. Iwuoha, *ChemElectroChem* **2024**, *11*, 1.
[28] K. C. Januarie, M. Oranzie, U. Feleni, E. Iwuoha, *Electrochim. Acta* **2023**, *463*, 142825.
[29] N. I. Khan, A. G. Maddaus, E. Song, *Biosensors* **2022**, *8*, 1.
[30] Y. Ma, J. Yang, T. Yang, Y. Deng, M. Gu, M. Wang, R. Hu, Y. Yang, *RSC Adv.* **2020**, *10*, 9723.
[31] M. A. Tabrizi, P. Acedo, *Nanomaterials* **2022**, *12*, DOI 10.3390/nano12030415.
[32] M. Jarczewska, J. Rębiś, Ł. Górski, E. Malinowska, *Talanta* **2018**, *189*, 45.
[33] S. Dong, D. Zhang, H. Cui, T. Huang, *Sens. Actuators B* **2019**, *284*, 354.
[34] M. Li, X. Xia, S. Meng, Y. C. Ma, T. Yang, Y. Yang, R. Hu, *RSC Adv.* **2021**, *11*, 6699.
[35] S. Jampasa, W. Siangproh, R. Laocharoensuk, T. Vilaivan, O. Chailapakul, *Talanta* **2018**, *183*, 311.
[36] H. J. Yang, M. W. Kim, C. V. Raju, C. H. Cho, T. J. Park, J. P. Park, *Biosens. Bioelectron.* **2023**, *234*, 115382.
[37] H. Gao, Y. Bai, B. He, C. S. Tan, *Biosensors* **2022**, *12*, 180.

Manuscript received: December 2, 2024
Revised manuscript received: January 2, 2025
Version of record online: February 9, 2025